JOURNAL OF APPLIED PHYSICS 98, 024106 (2005)

Dielectric properties of $Pb_{0.5}Ca_{0.5}TiO_3$ thin films

J. Mendiola[a] and R. Jiménez
Instituto de Ciencia de Materiales de Madrid, Consejo Superior de Investigaciones Científicas (CSIC), Cantoblanco, 28049 Madrid, Spain

P. Ramos
Instituto de Ciencia de Materiales de Madrid, Consejo Superior de Investigaciones Científicas (CSIC), Cantoblanco, 28049 Madrid, Spain and Departamento de Electrónica, Universidad de Alcalá, Alcalá de Henares, E-28871 Madrid, Spain

C. Alemany, I. Bretos, and M. L. Calzada
Instituto de Ciencia de Materiales de Madrid, Consejo Superior de Investigaciones Científicas (CSIC), Cantoblanco, 28049 Madrid, Spain

(Received 20 January 2005; accepted 29 May 2005; published online 22 July 2005)

A dielectric study is carried out on chemical solution-deposited calcium lead titanate (Pb,Ca)TiO_3 thin films, with calcium contents of 50 at. %, by measuring capacitance versus voltage as a function of temperature. A moderate ferroelectric activity is observed that remains in a broad temperature range, and that depends on the applied voltage and thickness of the films. This behavior is associated with the built-in fields generated as result of the space charge inside the films. From the diffusivity of dielectric constant versus temperature ($K'-T$) curves, the relaxorlike nature of the films is also demonstrated. The feasibility of these films for fabrication of voltage tuneable capacitors and charge store devices (dynamic random access memories) is confirmed. © *2005 American Institute of Physics*. [DOI: 10.1063/1.1984072]

I. INTRODUCTION

During the last years perovskite thin films such as $Ba_xSr_{1-x}TiO_3$ have been intensively investigated for its use in many applications requiring high charge storage densities in thin-film capacitors[1] and high dielectric nonlinearity for microwave (MW) devices.[2] These high permittivity materials are used as an alternative to the current SiO_2 or silicon oxide/nitride layers ("ONO"), whose thickness cannot be reduced beyond certain quantum limit, which is larger than the otherwise necessary to fabricate ultrahigh-density dynamic random access memories (DRAMs).[3]

Concerning the study of the classical $PbTiO_3$ perovskite, since the 1980s up to today, different modified $PbTiO_3$ compositions have been tested, starting by doping with diverse cations, by replacing Pb in the A site of the ABO_3 structure, to improve mainly piezoelectric and pyroelectric properties of bulk ceramic materials, as is described in Refs. 4–6. Pb has been substituted up to 50% for isovalent cations or rare earths, obtaining the highest performances for piezoelectric transducers in the case of doping with a 24% Ca instead of Pb. Rarely, doping has exceeded this amount. The main structure features reported were the reduced ferroelectric-paraelectric phase-transition temperature and the diminishing of the tetragonality up to $x=50\%$ in $Pb_{1-x}Ca_xTiO_3$. Close to $x=50\%$ and beyond, the composition-temperature phase diagram results to be more complicated, by appearing a superlattice with orthorhombic symmetry with properties that remind a ferroelectric relaxor.[7,8]

Another way to approach the $Pb_xCa_{1-x}TiO_3$ composition is from the other side of the solid solution, the $CaTiO_3$. Lemanov *et al.*[9] reported on $CaTiO_3$ as an incipient ferroelectric with a polar soft mode that may change by a small doping of Pb. The maximum of dielectric constant versus temperature ($K'-T$) appears for $x \geqslant 0.28$, that means the material shows a ferroelectric transition, from a polar phase to the centrosymmetric phase, *Pbnm*. This is the former structure of $CaTiO_3$ up to 1473 K,[10] which is responsible of superlattice reflections in these compositions, up to $x \sim 0.65$,[5] according to the octahedral tilting model reported by Glazer.[11] These transitions have been reported as relaxorlike in Refs. 9, 12, and 13 since a shift of the temperature at the maximum dielectric constant, T_m, with frequency is measured that fits the Vogël-Fulcher law and, a reduced dielectric frequency dispersion above T_m is also shown. From the experimental values reported for $Pb_xCa_{1-x}TiO_3$ bulk ceramics and thin films (see references therein and Refs. 12 and 14), the superlattice phase, *Pbnm* does not change abruptly into the tetragonal phase as the Pb amount increases at the expense of Ca. As Lemanov *et al.*[9] suggested, a morphotropic phase boundary (MPB) as a mixture of the orthorhombic paraelectric *Pbnm* phase and the ferroelectric *P4mm* phase should coexist for $0.45 < x < 0.55$. This is further experimentally confirmed by Chandra and Pandey in Ref. 15 by x-ray-diffraction (XRD) analysis (the two phases coexist in the range for $0.4 \leqslant x \leqslant 0.6$). Outside the MPB, the temperature phase transition, from ferroelectric, *P4mm*, to the paraelectric cubic phase, *Pm3m*, increases linearly with the amount of Pb substituted by Ca, as reported in Refs. 16 and 17.

Among the scarce publications on $Pb_{0.5}Ca_{0.5}TiO_3$ thin films, the authors of this work have previously reported preliminary results on high dielectric properties of these thin-film materials.[18,19] The aim of this paper is to progress into the knowledge of the $Pb_{0.5}Ca_{0.5}TiO_3$ solid solution, as a thin

[a]Electronic mail: mendiola@icmm.csic.eg

film form onto $Pt/TiO_2/SiO_2/(100)Si$ substrates, on the basis of their dielectric properties. Models for dielectric properties of polycrystalline ferroelectric thin films are lacking. Majority of the works on films that make use of the Landau-Ginzburg-Devonshire (LGD) phenomenological thermodynamic model are only for epitaxial films,[20–22] to justify dielectric properties,[23–25] including residual stresses produced by the processing. This model should not be applied to polycrystalline films.

Meanwhile, because the potential applications of these films deal with applied external voltages we propose in this work the use of the well-known experimental technique of measuring capacitance versus voltage ($C-V$) at several temperatures, to get information on the dielectric nature of the films, such as electric bias effects on the transition temperature, thickness dependence of nonlinearity, and dielectric diffusivity of transition. Finally, feasibility of the films for fabrication of voltage tunable capacitors and charge storage devices (DRAMs) is also evaluated.

II. EXPERIMENTAL PROCEDURES

Calcium-modified lead titanate precursor solutions with nominal composition of $Pb_{0.5}Ca_{0.5}TiO_3$ synthesized by a sol-gel method,[26] were spin coated onto $Pt/TiO_2/SiO_2/(100)Si$ substrates. Crystallization of the films was carried out by rapid thermal processing (RTP). Crystal structure and texture were controlled by x-ray diffraction. Three films, ~100, ~295, and ~520 nm thick, were prepared. Dot Pt/Au electrodes of 2×10^{-3}-cm^2 area and 50 nm thick were deposited by sputtering on the films surfaces using a shadow mask to get an array of capacitors that permits to perform dielectric measurements. Capacitance versus bias voltage, $C-V$, has been measured for a wide temperature range with intervals of 5 K at 10 kHz with an impedance analyzer, HP 4194A. $C-V$ measurements were performed in the films by biasing the capacitor with changing bias in a staircase way, while measuring the high-frequency capacitance in a stationary state with a small signal amplitude (0.01 V). Measurements were carried out by sweeping with the bias in both directions searching for hysteresis as a function of temperature. Leakage current densities were measured for the thickest film in the electric-field range employed by using a pulse generator HP 8116A and an electrometer Keithley 6514. In the thinnest film, testing of voltage drop of the capacitor after a pulse was performed by means of a homemade data acquisition set up. The setup sampled the voltage level of the capacitor by a data acquisition hardware, DAQ, after applying a pulse of 3 V of amplitude for 4 ms. Its input impedance was 100 GΩ and sampling rates up to 2×10^5 samples/s with 16-bit accuracy. The measurement tasks were programmed by the commercial LABVIEW software. A single-phase bulk ceramic of the same composition than the films and with an average grain size around 1 μ was fabricated by the conventional ceramic method. Dielectric constant with temperature at 10 kHz at room temperature was measured on this ceramic sample to compare with the dielectric results of thin films.

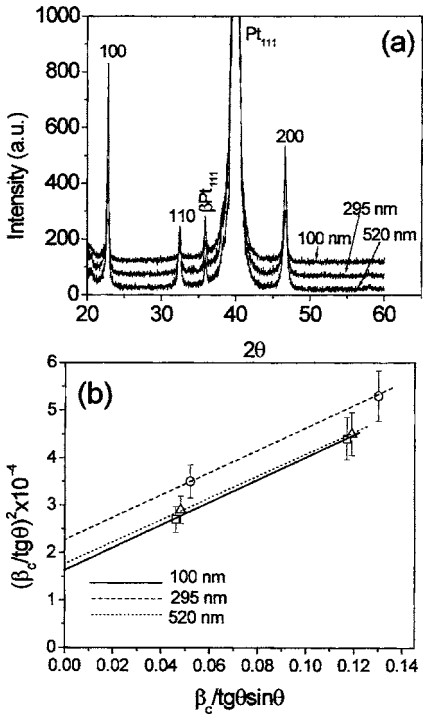

FIG. 1. (a) XRD patterns, θ-2θ scans of the 100-, 295-, and 520-nm-thick films. Peaks with label 100, 110, and 200 correspond to the single PTCa50 perovskite phase. The strong 111 peaks of the high-oriented platinum bottom substrate are observed for Kα and β wavelengths. (b) Mean microstrains and crystallite sizes are deduced from the straight lines obtained by fitting with Eq. (1).

III. RESULTS AND DISCUSSION

Single pseudocubic phase is observed by x-ray diffraction, with a high ⟨100⟩-preferred orientation (see Fig. 1). No change in the lattice parameters is measured with the film thickness, neither through the cross section. Applying the integral breadths method to the broadening Bragg lines 100 and 200 of the XRD patterns [see Fig. 1(a)], microstrains and effective crystallite size are calculated. According to Ref. 27,

$$(\beta_T/tg\,\theta)^2 = (K\lambda/\langle D\rangle)(\beta_T/tg\,\theta\sin\theta) + 16\langle\varepsilon\rangle^2, \qquad (1)$$

where β_T is the total integral breath, λ the Cu Kα wavelength, $\langle D\rangle$ the mean effective crystallite size, and $\langle\varepsilon\rangle$ the mean microstrains. Microstrains and grain size are calculated from the slope and the ordinate intercept of the fit straight lines [Fig. 1(b)]. Since the estimated error of β_T is ±5%, the same values of microstrains $\langle\varepsilon\rangle\approx3.5\times10^{-3}\pm5\%$ and grain sizes $\langle D\rangle\approx60\pm10\%$ nm are obtained for the three films. Grain sizes calculated agree well with that deduced from previous atomic force microscopy (AFM) results of the authors[26] (50 nm). Figure 2 shows the $C-V$ measurements of the three films at three discrete and very different temperatures, selected for clarity. Due to the measuring technique, these loops do not inform on charge contribution of domain switching, but for other polar elements, according to Brenann.[28] The asymmetry of the loops around zero voltage bias with different maximum values shows the existence of charge carriers (oxygen vacancies) at the film electrode interfaces that are of different nature due to the film and capacitor fabrication process. Besides this effect, we observe

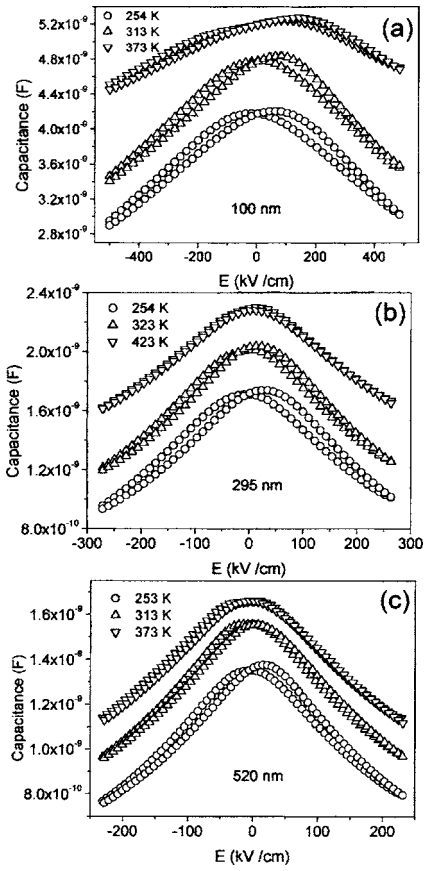

FIG. 2. $C-V$ measurements at three separate temperatures. The two higher temperatures capacitance values are displaced for clarity. (a) 100 nm thick. Data displacement: 313 K$+0.5\times10^{-9}$ F and 373 K$+1\times10^{-9}$ F, (b) 295 nm thick. Data displacement: 323 K$+0.2\times10^{-9}$ F and 423 K$+0.6\times10^{-9}$ F. (c) 520 nm thick. Data displacement: 313 K$+0.15\times10^{-9}$ F and 373 K$+0.3\times10^{-9}$ F. Hysteresis remains for the thinnest film even at 373 K.

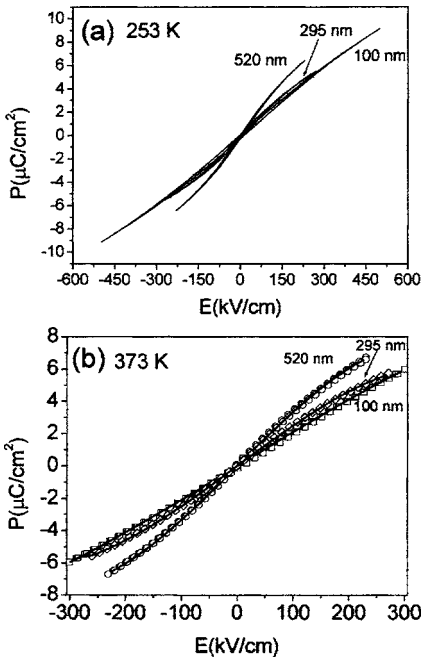

FIG. 3. Comparison of $P-E$ loops obtained by integration of $C-V$ curves of the three films (a) at 253 K and (b) at 373 K. Nonlinearity is significantly larger for the thickest film; the merged continuous line (only one branch) shows the good fitting with Eq. (2).

noteworthy differences between the three $C-V$ sets. For the two thickest films, the two branches are practically undistinguishable above certain temperature, well above that corresponding to the phase transition of a counterpart bulk ceramic; that is to say, ferroelectric behavior is weak but remains up to at least this temperature. However, the two branches continue being separated even at 373 K for the thinnest film, indicating a residual hysteresis behavior, related with polarization stabilization. Figure 3, compare the hysteresis loops calculated for the three films by integrating the $C-V$ curves obtained at the lowest applied bias voltage, for two extreme temperatures: at 253 K (ferroelectric phase) and at 373 K (well above the maximum of K'). In these calculations, P is taken as the induced polarization since it does not include switching contributions, but informs us about domain-wall dynamic. This confirms the reduced but still polar nature of these films well above T_m. The loops are more slanted for the thinnest than for the thickest film; that means polarizability increases drastically with film thickness. Furthermore, nonlinearity of P versus electric field, E, clearly increases with the film thickness. Since the two branches of the loops are very similar, even at low temperatures, we have only taken one of the branches for our calculations, and the typical S shape of a $P-E$ behavior in the paraelectric state is obtained. These curves fit to the expression,

$$P = aE - bE^3, \tag{2}$$

where a and b are coefficients, P is the induced polarization, and E the applied electric field. This equation is fulfilled in a system with a centrosymmetrical paraelectric state at temperatures over the Curie temperature ($T>T_c$). Here, values of the linear coefficient a are 2.1×10^{-9}, 2.5×10^{-9}, and 3.4×10^{-9} C m^{-1} V^{-1}, for the 100-, 295-, and 520-nm-thick films, respectively. This parameter defines the slant degree of the hysteresis loop and corresponds to the permittivity value. The calculated b coefficient of the thickest film is an order of magnitude larger than that of the thinnest one. These values are 1.19×10^{-25}, 6.35×10^{-25}, and 1.06×10^{-24} C m V^{-3} for the 100-, 295-, and 520-nm-thick films, respectively. This means nonlinearity increases with the film thickness, and therefore the thickest film should show a higher tunability, as it will be discussed below. From the $C-V$ data obtained at several temperatures, we can also draw the evolution of dielectric constant with temperature, $K'-T$, at different applied bias fields (Fig. 4). A family of decreasing $K'-T$ curves is observed as the applied external bias increases. For the 520- and 295-nm-thick films, the temperature of maximum, T_m, shifts to higher values with the increase of applied bias field, meanwhile for the other film it remains approximately at the same T_m value. Figure 5 shows a T_m dependence on the external bias for the 520-nm-thick film that results in a linear relation with a slope of $\Delta T_m/\Delta E_b$ of $\sim$0.6 K/kV cm^{-1}. This is the expected behavior for a ferroelectric material, according to the expression

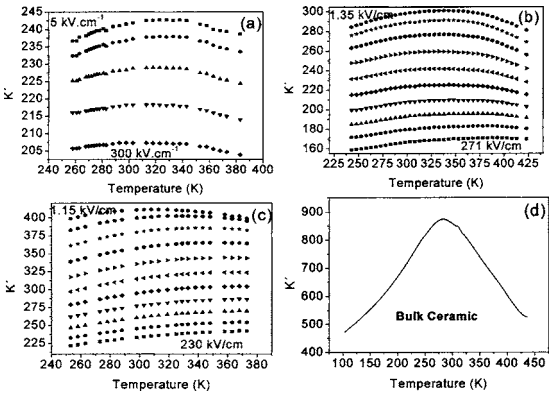

FIG. 4. Variation of $K'-T$ as a function of the external bias field for the (a) 100-nm, (b) 295-nm, and c) 520-nm-thick films. For comparison see the $K'-T$ curve (d) of a bulk ceramic with the same composition but with a larger grain size. The shift of the maximum, T_m, to higher temperatures as the external bias increases can be observed, but that remain fixed for the 100-nm-thick film.

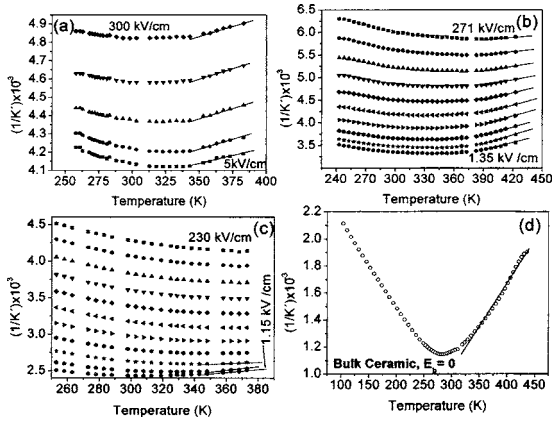

FIG. 6. Temperature variation of $1/K'$ as a function of external bias field of a) 100-, b) 295-, and c) 520-nm-thick films. Note the Curie-Weiss-like behavior differences with film thickness. For comparison, see the $1/K'-T$ curve (d) of a bulk ceramic with the same composition but larger grain size, showing the approximate Curie-Weiss-like behavior.

$$\Delta T_c/\Delta E = 2/\beta \Delta D, \tag{3}$$

being β the inverse of the Curie-Weiss constant and D the electric displacement, according to Ref. 29. Figure 4 also shows that for the thickest film, beyond a high E value, the curves $K'-T$ become very broad, being the maximum undistinguishable. This means polar activity is practically absent. This is more clearly shown in the graphic of the inverse $1/K'$ vs T of Fig. 6. Despite the experimental rounded maximum $K'-T$, certain linearity can be observed above T_m that remind a Curie-Weiss-like behavior. That is exhibited for values of bias from 0 to ~100 kV/cm in the 520-nm-thick film, but with decreasing slopes to K' values practically temperature independent. The behavior of the thinnest film is different [Fig. 6(a)] since the moderate small slope remains stable up to the highest applied electric bias without a noticeable T_m shift. This film offers a strong resistance to the shifting of T_m by an external bias. The strains generated in the films during processing and their microstructure (grain size) are sometimes invocated as causes of K' reduction in thin films,[30,31] but in this work, as described before, grain size and strains are similar in the three films. Therefore, other causes must be explored. The described resistance to maintain T_m in the thinnest film can be associated with its small thickness, probably through the built-in field generated as a result of the space charge inside the film. Assuming charged defects into the films (mainly, oxygen vacancies), these defects have to be majority placed close to the bottom electrode interface, more than in the proximity of the top electrode, due to the processing conditions. Charge concentration will increase with decreasing film thickness[32] and therefore strong asymmetric built-in fields will be generated in very thin films, raising the coercive field of both signs. From $C-V$ curves, internal bias fields of 22.5, 13.5, and 3.8 kV/cm are calculated for the 100-, 295-, and 520-nm-thick films, respectively. Nevertheless, we suspect that the lower the thickness of the film, the higher the built-in fields that would impede switching polarization and therefore, should be the cause of the maintenance of the T_m values against the external bias and the smaller K' values in the thinnest film.[32]

$C-V$ measurements with temperature also provide the way to prove that the broadening of maximum $K'-T$ (diffusivity) could be a consequence of the relaxorlike nature of the films. To study the diffuse phase transition in thin films, we have used the following approach of Uchino and Nomura:[33]

$$1/K'(T) = 1/K'_m[1 + (T - T_m)^{\gamma}/2\Delta^2]. \tag{4}$$

Equation (4) is fulfilled in the vicinity of a diffuse phase transition for any frequency, being $\gamma=2$ for a relaxorlike be-

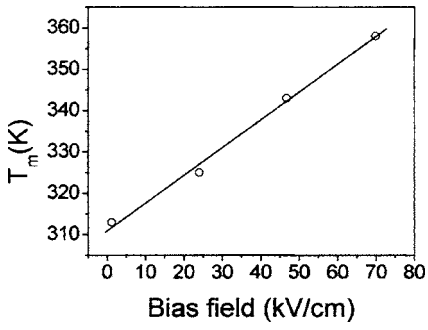

FIG. 5. Shift of T_m as a function of external bias field for the 520-nm-thick film. This follows a straight line, as expected for a ferroelectric material (Ref. 29). Above 70 kV/cm, T_m is difficult to distinguish due to the high broadening.

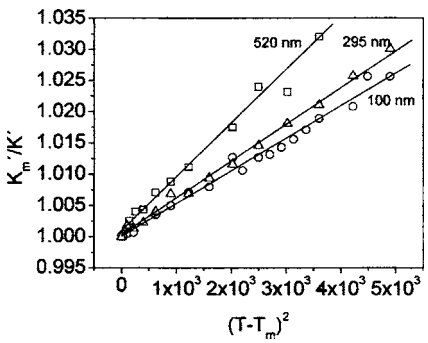

FIG. 7. Diffuse phase-transition behavior. Linear fitting of K'_m/K' vs $(T-T_m)^2$ with Eq. (3) shows the relaxorlike nature of the films. Diffusivity increases as the film thickness is reduced.

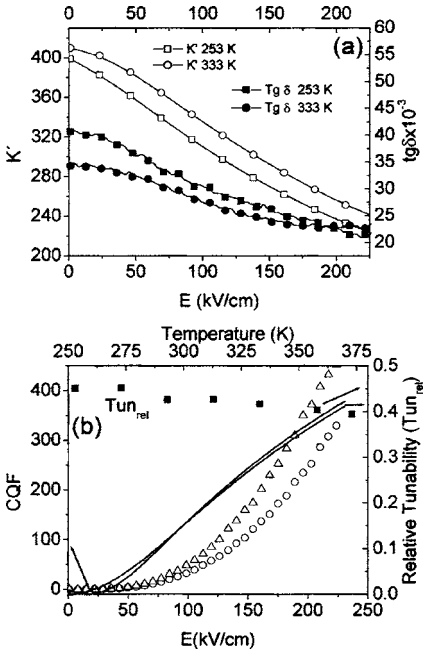

FIG. 8. (a) Variation of $K'-E$ and $tg\ \delta-E$ of the 520-nm-thick film for two separate temperatures, 253 and 333 K. (b) $\mathrm{Tun_{rel}}$ for $V_{\max}$ as a function of temperature and variation of commutation quality factor, CQF and $\mathrm{Tun_{rel}}$ with bias field, at 253 and 333 K.

havior and Δ the broadening parameter. By using the plotting of K'_m/K' vs $(T-T_m)^2$, the linear relation is reasonably fulfilled for the three films. Figure 7 shows straight-line fittings for the three films, thus confirming the relaxorlike character previously reported by the authors.[18] The slope for the 520-nm-thick film is larger than those of the other films, which gives us information about the less diffusivity degree in the former. The formal contradiction between the relaxor nature and Curie-Weiss behavior deduced from the experimental results could be due to the fact that the present composition corresponds to the above-suggested morphotropic phase boundary where two phases coexist. Further measurements at higher resolution are needed to solve the issue.

From the application point of view, the analysis of $C-V$ measurements allows us to evaluate the feasibility of these films for high-frequency devices through calculations of their tunability as a function of temperature (the degree of variation of the dielectric constant or capacitance as a function of the applied electric field). Relative tunability, $\mathrm{Tun_{rel}}$, is defined by,

$$\mathrm{Tun_{rel}} = (C_{\max} - C_{\min})/C_{\max}, \tag{5}$$

where $C_{\max}$ and $C_{\min}$ are the values of maximum and minimum of capacitance corresponding to the minimum and maximum of applied voltages. But for applications, the parameter that combines tunability with loss tangent results more realistic. That is the commutation quality factor (CQF), given by

$$\mathrm{CQF} = (T_r - 1)^2/T_r tg\,\delta_1 \cdot tg\,\delta_2, \tag{6}$$

being $tg\,\delta_1$ and $tg\,\delta_2$ the tangent of losses for the minimum and maximum of the applied voltage and T_r the ratio between $C_{\max}$ and $C_{\min}$. Figure 8(a) gives a general behavior of the dielectric constant, K', and the loss tangent, $tg\,\delta$, as a function of the applied electric field for the thickest film at two temperatures, 253 and 333 K. This film has been selected because of its large nonlinearity compared with the other two films that results from the previous analysis of P vs E. A change larger than 1.6 times of K' at $V_{\min}$ in the measured range means a reasonable good tunability. This change is shown in Fig. 8(b), where relative tunability versus electric field grows up to 45%. The values of $\mathrm{Tun_{rel}}$ for $V_{\max}$ as a function of temperature also show a moderate decrease in a range of temperature of 140 K. Despite the moderate values of $tg\,\delta$, those have not been corrected by the contribution of the electrode resistance (expected small for low-frequency range), the variation of the CQF parameter as a function of the applied electric field for temperatures of 253 and 333 K seems to be adequate for tunable applications. CQF values are quite similar and close to 200 up to an applied electric field of 175 kV/cm. Although microwave applications require additional measurements at higher frequencies with interdigital electrodes (IDEs), we estimate in a first approach, that the low-frequency measurements here reported with a parallel-plate electrode configuration can provide a suitable method to characterize these films for integrated voltage-tunable devices (varactors). This is true for a normal ferroelectric (see a recent review of Tagantsev[34]), but not for a relaxor ferroelectric. However, despite the relaxor nature of the films of this work, the reported frequency dispersion occurs for temperatures up to the maximum of K', but not beyond that because the shift of T_m with frequency is small. Therefore, the results here obtained are promising to considerate these thin films as good candidates in MW applications.

Since the capacitor must be charged from zero to V, the $C-V$ curves also inform us about the capability of these thin films for the DRAMs. The demand from the material used in these devices should be a high dielectric constant to get a high capacitance density and low leakage density current to retain its voltage once the capacitor is charged up. For the thinnest film of this work, more appropriate for high-density memories, a charge of about 9×10^{-9} C is involved in the broad temperature range of 253–333 K, where variations less than 5% are measured and a capacitance density close to 15 fF/μ^2 is obtained. This means an equivalent of an ~4-nm-thick ONO layer. In accordance with the current recommendations,[35] the ability of voltage retain of a small capacitor must be larger than 90%. This is fulfilled for the thinnest film of this work; see values shown in Fig. 9 for the 100-nm-thick film. The voltage drop after 200 ms (the usual refreshment time in a DRAM) is less than 5%. These results contribute to the reduced leakage current densities measured in the film, which are lower than 10^{-7} $\mathrm{A/cm^2}$ at 3 V.

IV. CONCLUSIONS

The $C-V$ measuring technique has proved to be suitable to study the dielectric behaviour of $Pb_{0.5}Ca_{0.5}TiO_3$ thin films with different thickness.

Dielectric constant versus temperature $(K'-T)$ curves of these films shows a large diffusivity from which the relaxor-

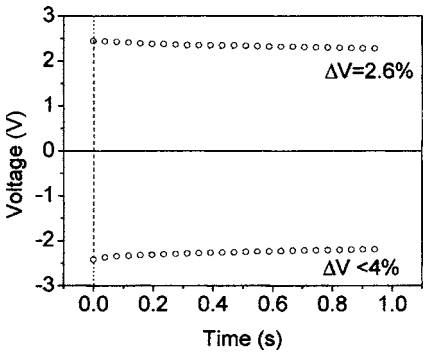

FIG. 9. Time voltage drop after writing pulse in the 100-nm-thick film for the two signs of voltage charge.

like nature is confirmed for any film thickness. By integrating $C-V$ loops, a weak polar activity is observed in the films up to temperatures well above the temperature of the maximum dielectric constant, T_m. Films with thickness ~100 nm offer a strong resistance to the shift up of T_m by an external bias. An increase of space charge density into the films by decreasing thickness is suggested as the cause of the reduction of K' and also as responsible of the fixed T_m with the applied voltage in the thinnest film, due to the built-in fields generated into the films.

The high tunability measured at 10 kHz (40%–50%) in a broad temperature range of a 520-nm-thick film suggests the feasibility of these films for MW devices application. Films with thickness below ~100 nm are shown as a chance for DRAM fabrication. They have a high capacitance density ($\sim 15\ \mathrm{fF}/\mu^2$), a low leakage current density ($<10^{-7}\ \mathrm{A/cm^2}$ at 3 V) and an ability to retain above the 95% of the written voltage after 200 ms.

ACKNOWLEDGMENTS

This work has been supported by the Spanish Project No. MAT2001-1564. One of the authors (R.J.) recognizes the support of Ramon y Cajal contract of the Ministerio de Educación y Ciencia.

[1]A. I. Kingon, S. K. Streiffer, C. Basceri, and S. R. Summerfelt, Mater. Res. Bull. **21**, 46 (1996).
[2]A. Kozyvev, A. Ivanov, T. Samoilova, O. Soldatenkov, K. Astafiev, and L. C. Sengupta, J. Appl. Phys. **88**, 5334 (2000).
[3]A. I. Kingon, J. P. Maria, and S. K. Streiffer, Nature (London) **406**, 1020 (2000).
[4]Y. Yamashita, K. Yokoyama, H. Honda, T. Takahashi. Jpn. J. Appl. Phys., Suppl. **20**, 183 (1981).
[5]T. Yamamoto, M. Saho, and K. Okazaki, Jpn. J. Appl. Phys., Suppl. **26**, 57 (1987).
[6]J. Mendiola, B. Jiménez, C. Alemany, L. Pardo, and L. Del Olmo, Ferroelectrics **94**, 183 (1989).
[7]V. V. Eremkin, V. G. Smotrakov, S. I. Shevtsova, and A. T. Kozakov, Phys. Solid State **36**, 191 (1994).
[8]R. Ganesh and E. Goo, J. Am. Ceram. Soc. **80**, 653 (1997).
[9]V. V. Lemanov, A. V. Sotnikov, E. P. Smirnova, and M. Weihnacht, Appl. Phys. Lett. **81**, 886 (2002).
[10]B. J. Kennedy, C. J. Howard, and B. C. Chakoumakos, J. Phys.: Condens. Matter **11**, 1479 (1999).
[11]A. M. Glazer, Acta Crystallogr., Sect. A: Cryst. Phys., Diffr., Theor. Gen. Crystallogr. **31**, 756 (1975).
[12]J. Mendiola, C. Alemany, R. Jimenez, E. Maurer, and M. L. Calzada, Bol. Soc. Esp. Ceram. Vidrio **43**, 620 (2004).
[13]R. Ranjan, N. Singh, D. Pandey, V. Siruguri, P. S. R. Krishna, S. K. Paranjpe, and A. Banaerjee, Appl. Phys. Lett. **70**, 3221 (1997).
[14]J. Mendiola and M. L. Calzada, in *Handbook of Thin Films Materials*, edited by H. S. Nalva (Academic, San Diego, 2002), p. 369.
[15]A. Chandra and D. Pandey, J. Mater. Res. **81**, 407 (2003).
[16]J. Mendiola, B. Jiménez, C. Alemany, L. Pardo, and L. Del Olmo, Ferroelectrics **94**, 183 (1989).
[17]R. Ganesh and E. Goo, J. Am. Ceram. Soc. **80**, 653 (1997).
[18]R. Jimenez, C. Alemany, M. L. Calzada, and J. Mendiola, Ferroelectrics **302**, 461 (2004).
[19]J. Mendiola, R. Jimenez, P. Ramos, C. Alemany, M. L. Calzada, and E. Maurer, Bol. Soc. Esp. Ceram. Vidrio **43**, 445 (2004).
[20]G. A. Rossetti, Jr, L. E. Cross, and K. Kushida, Appl. Phys. Lett. **59**, 2524 (1991).
[21]N. A. Perstev, A. G. Zembilgotov, and A. K. Tagantsev, Phys. Rev. Lett. **80**, 1988 (1998).
[22]S. K. Streiffer, C. Basceri, C. B. Parker, S. E. Lash, and A. I. Kingon, J. Appl. Phys. **86**, 4565 (1999).
[23]N. A. Pertsev, A. G. Zembilgotov, and A. K. Tagantsev, Phys. Rev. Lett. **80**, 1988 (1998).
[24]S. P. Alpay and A. L. Roytburd, J. Appl. Phys. **83**, 4714 (1998).
[25]L. Chen, V. Nagarajan, R. Armes, and A. L. Roitburd, J. Appl. Phys. **94**, 147 (2003).
[26]I. Bretos, J. Ricote, R. Jiménez, J. Mendiola, and M. L. Calzada, Integr. Ferroelectr. **61**, 105 (2004).
[27]H. P. Klug and L. E. Alexander, *X-Ray Diffraction Procedures*, 2nd ed. (Wiley, New York, 1974).
[28]C. Brennan, Integr. Ferroelectr. **8**, 335 (1995).
[29]M. E. Lines and A. M. Glass, *Principles and Applications of Ferroelectrics and Related Materials* (Clarendon, Oxford, 1977).
[30]W. J. Lee, A. L. Roitburd, S. P. Alpay, T. D. Trau, L. Salamanca-Riva, R. Ramesh *et al.*, J. Appl. Phys. **80**, 5891 (1996).
[31]M. B. Kelman, L. F. Schloss, P. C. McIntyre, B. C. Hendrix, S. M. Bilodeau, and J. F. Roeder, Appl. Phys. Lett. **80**, 1258 (2002).
[32]C. H. Lin, P. A. Friddle, C. H. Ma, A. Daga, and H. Chen, J. Appl. Phys. **90**, 1509 (2001).
[33]K. Uchino and S. Nomura, Ferroelectrics **44**, 55 (1982).
[34]A. K. Tagantsev, V. O. Sherman, K. F. Astafiev, J. Venkatesh, and N. Setter, J. Electroceram. **11**, 5 (2003).
[35]S. Hoffman and R. M. Waser, Integr. Ferroelectr. **17**, 141 (1997).